JOURNAL OF BACTERIOLOGY, June 2005, p. 4245–4256 Vol. 187, No. 12
0021-9193/05/$08.00+0 doi:10.1128/JB.187.12.4245–4256.2005

Overproduction of CcmG and CcmFH$_{Rc}$ Fully Suppresses the *c*-Type Cytochrome Biogenesis Defect of *Rhodobacter capsulatus* CcmI-Null Mutants

Carsten Sanders,[1] Meenal Deshmukh,[1]† Doniel Astor,[1] Robert G. Kranz,[2] and Fevzi Daldal[1]*

Department of Biology, Plant Science Institute, University of Pennsylvania, Philadelphia, Pennsylvania 19104,[1] and Department of Biology, Washington University, St. Louis, Missouri 63130[2]

Received 12 January 2005/Accepted 11 March 2005

Gram-negative bacteria like *Rhodobacter capsulatus* use intertwined pathways to carry out the posttranslational maturation of *c*-type cytochromes (Cyts). This periplasmic process requires at least 10 essential components for apo-Cyt *c* chaperoning, thio-oxidoreduction, and the delivery of heme and its covalent ligation. One of these components, CcmI (also called CycH), is thought to act as an apo-Cyt *c* chaperone. In *R. capsulatus*, CcmI-null mutants are unable to produce *c*-type Cyts and thus sustain photosynthetic (Ps) growth. Previously, we have shown that overproduction of the putative heme ligation components CcmF and CcmH$_{Rc}$ (also called Ccl1 and Ccl2) can partially bypass the function of CcmI on minimal, but not on enriched, media. Here, we demonstrate that either additional overproduction of CcmG (also called HelX) or hyperproduction of CcmF-CcmH$_{Rc}$ is needed to completely overcome the role of CcmI during the biogenesis of *c*-type Cyts on both minimal and enriched media. These findings indicate that, in the absence of CcmI, interactions between the heme ligation and thioreduction pathways become restricted for sufficient Cyt *c* production. We therefore suggest that CcmI, along with its apo-Cyt chaperoning function, is also critical for the efficacy of holo-Cyt *c* formation, possibly via its close interactions with other components performing the final heme ligation steps during Cyt *c* biogenesis.

The *c*-type cytochromes (Cyts) are ubiquitous proteins that function as electron carriers between various energy transduction complexes in major metabolic pathways like photosynthesis (Ps) and respiration (Res). They contain heme (iron protoporphyrin IX) molecules as prosthetic groups that are covalently attached via thioether bonds formed between the vinyl groups of the heme moiety and the cysteine thiol groups of a conserved signature motif (almost exclusively Cys-Xxx-Yyy-Cys-His) within apo-Cyt *c* (46). Three distinct posttranslational maturation processes are known for the production of *c*-type holo-Cyts in prokaryotic and eukaryotic organisms (35, 43). Plant and most protozoan mitochondria, *Archaea*, and many gram-negative bacteria use system I, depicted in Fig. 1, top. It consists of at least 10 essential membrane-bound components that chaperone the *c*-type apo-Cyts to the maturation sites after their translocation across the cytoplasmic membrane, reduce the disulfide bonds between the cysteines of their heme binding motifs, export the heme cofactors into the periplasm, and attach them covalently and stereospecifically to the apo-Cyts (2, 35, 43, 60, 61).

The gram-negative, purple nonsulfur facultatively photosynthetic bacterium *Rhodobacter capsulatus* produces various soluble or membrane-bound *c*-type Cyts, including Cyts c_1, c_2, c', c_y, c_o, and c_p (14, 28, 33, 66), to sustain its versatile growth modes. Cyt c_1 and either Cyt c_2 or c_y are required for Ps growth (66), whereas Cyt c_o and c_p are essential subunits of the cbb_3-type Cyt *c* oxidase involved in Res growth (33). The activity of the latter enzyme can be directly detected by monitoring the staining of colonies following the Nadi (α-naphthol + dimethylphenylenediamine → indophenol blue + H_2O) reaction (32), Thus, *R. capsulatus* mutants unable to form *c*-type holo-Cyts can be identified by their Ps$^-$/Nadi$^-$ dual phenotype (34), via which essential components of Cyt *c* biogenesis have been identified in this species (Fig. 1, top) (4, 5, 7, 15, 26, 38). As in *Escherichia coli*, the CcmABCD (also called HelABCD) components form an ATP-binding cassette (ABC)-containing transporter complex, thought to be involved in the export of the heme cofactor across the cytoplasmic membrane. The exported heme binds to CcmE (also called CycJ) (54), which conveys it to the putative apo-Cyt *c* heme lyase component CcmF (also called Ccl1) (25–27). Unlike *E. coli*, *R. capsulatus* and some other species contain two additional components: CcmI (also called CycH), which is proposed to chaperone the *c*-type apo-Cyts to the maturation site following their translocation to the periplasm (5, 38), and a membrane-bound thioredoxin, designated here as CcmH$_{Rc}$ (also called Ccl2), which is involved in the apo-Cyt *c* thioreduction pathway (4, 5). In *E. coli*, the carboxyl-terminal part of CcmI is fused to the homologue of CcmH$_{Rc}$ to form CcmH (35, 43, 59) (referred to as CcmH$_{Ec}$ here).

As disulfide bonds are formed in the periplasm between the cysteines of translocated proteins via the DsbA/DsbB pathway for oxidative protein folding (11, 29), similar bonds are also assumed to be built between the heme binding cysteine thiols (39, 40, 50, 51). For periplasmic disulfide reduction, electrons originating from TrxA are thought to be shuttled across the cytoplasmic membrane via CcdA (homologous to the central

* Corresponding author. Mailing address: Department of Biology, Plant Science Institute, University of Pennsylvania, Philadelphia, PA 19104. Phone: (215) 898-4394. Fax: (215) 898-8780. E-mail: fdaldal@sas.upenn.edu.

† Present address: Colgate-Palmolive Inc. Research Center, Piscataway, N.J.

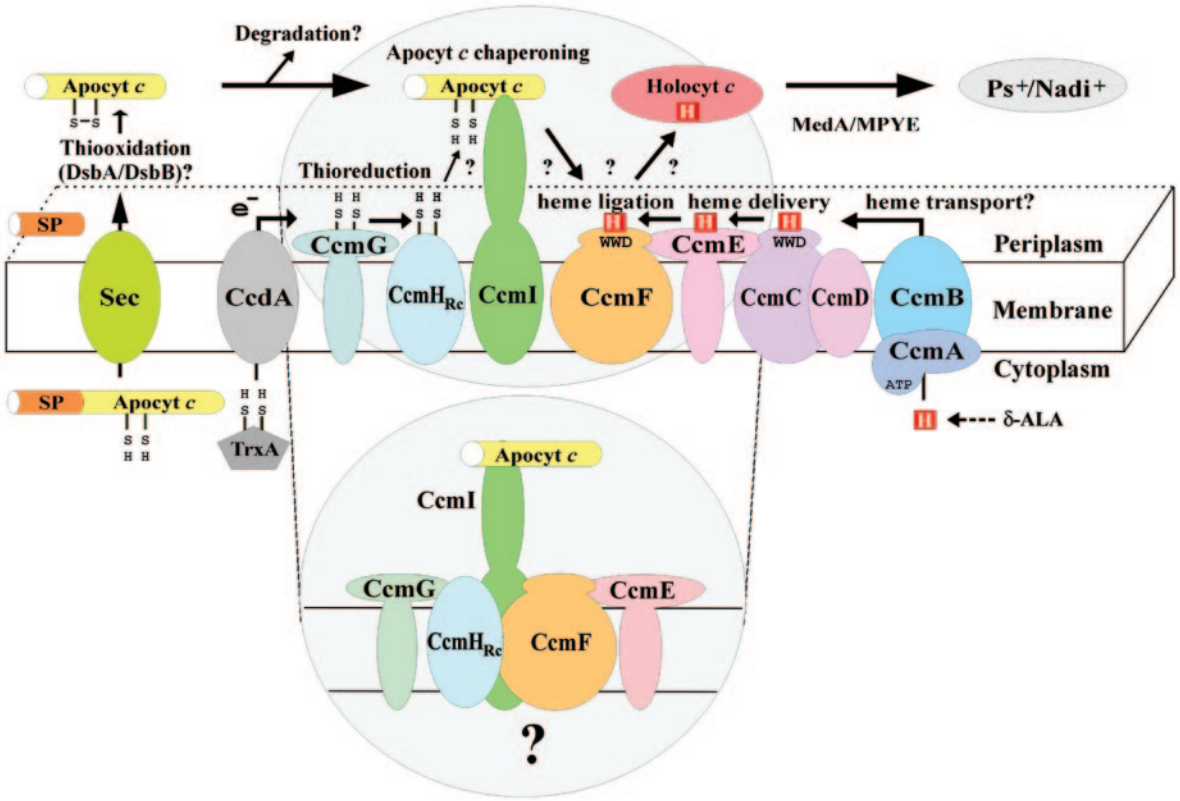

FIG. 1. Current model of Cyt *c* biogenesis in *R. capsulatus*. Pre-apo-Cyt *c* produced in the cytoplasm are translocated across the membrane via the Sec-dependent secretory pathway. Their signal peptides (SP) are either processed or used as N-terminal membrane anchors. Disulfide bonds are assumed to be formed within the cysteines of the conserved apo-Cyt *c* heme binding motif CxxCH and then possibly chaperoned via CcmI to the Cyt *c* maturation site. CcdA shuttles electrons across the membrane to the thioreduction component $CcmH_{Rc}$ via CcmG. $CcmH_{Rc}$ is thought to reduce the heme binding site disulfides prior to heme attachment. The heme cofactor (H) is synthesized in the cytoplasm from δ-amino levulinic acid (δ-ALA), putatively transported to the periplasm via the ATP-binding cassette (ABC) transporter CcmAB, and covalently ligated to CcmE via CcmCD, with WWD referring to the putative heme binding motif. CcmE is postulated to provide the heme to the putative heme lyase component CcmF, which is believed to attach it covalently and stereospecifically to the reduced apo-Cyt *c*. According to this model, CcmI-null mutants are not able to produce any holo-Cyt *c*, because apo-Cyt *c* is not delivered efficiently to the maturation site, as they probably are degraded rapidly. Hence, overproduction of CcmF and $CcmH_{Rc}$ can alleviate the need for apo-Cyt *c* chaperoning and protection function of CcmI. Arrows refer to electron (e-) transfer steps, and ? indicates hypothetical steps. The bottom portion depicts the proposed interactions between CcmI, CcmG, CcmF, $CcmH_{Rc}$ and CcmE, forming a hypothetical Cyt *c* biogenesis "core complex" in *Rhodobacter capsulatus*. This model proposes that apo-Cyt *c* interacts with CcmI as part of a multisubunit protein complex including CcmF and $CcmH_{Rc}$.

domain of *E. coli* DsbD) to CcmG (also called HelX) and then to $CcmH_{Rc}$ or $CcmH_{Ec}$ depending on the species. The disulfide bonds at the heme binding sites of the *c*-type apo-Cyts are then believed to be reduced by $CcmH_{Rc}$ (or $CcmH_{Ec}$) prior to covalent and stereo-specific heme ligation (Fig. 1, top) (15, 21–23, 30, 41, 44, 48, 56).

In *R. capsulatus*, CcmI is thought to act as a chaperone that delivers apo-Cyts to the maturation sites (38). Its sequence analysis indicates that it is a bipartite membrane protein that contains two amino-terminal transmembrane helices and a large periplasmic carboxyl-terminal extension of over 300 amino acids (38), designated CcmI-1 and CcmI-2, respectively. In *R. capsulatus* CcmI mutants lacking the CcmI-2 domain, *c*-type Cyt maturation becomes growth medium dependent. For example, they can still produce several *c*-type Cyts (e.g., Cyt c_1, c_p, and c_o) during growth in minimal medium but only Cyt c_1, which is a subunit of the Cyt bc_1 complex (14), in minimal and enriched media, indicating that CcmI-2 is not required for its maturation (38). Interestingly, *E. coli*, which does not contain a Cyt c_1 homologue, naturally lacks an equivalent of CcmI-1.

Our previous analysis of $Ps^+/Nadi^+$ revertants of *R. capsulatus* CcmI-null mutants, such as MT-SRP1.r1, indicated that overexpression of $ccmFH_{Rc}$ can bypass the function of CcmI during *c*-type Cyt maturation on minimal, but not on enriched, medium (16). Remarkably, these mutants can become fully proficient for Cyt *c* maturation on both media upon acquisition of additional mutations. In this work, we demonstrate that, in addition to the overexpression of $ccmFH_{Rc}$, either overexpression of *ccmG* or hyperexpression of $ccmFH_{Rc}$ is required to fully overcome the role of CcmI in minimal and enriched growth media. These findings indicate that, in the absence of CcmI, interactions between the thioreduction and heme ligation components become restricted, limiting adequate *c*-type Cyt production. Therefore, although CcmI is not essential for the attachment of the heme cofactor per se, it is an important component for sufficient holo-Cyt *c* formation under Res and Ps growth on minimal and enriched media.

MATERIALS AND METHODS

Bacterial strains, plasmids, and growth conditions. The bacterial strains and plasmids used in this work are described in Table 1. *R. capsulatus* strains were grown at 35°C on enriched (12) or minimal (57) medium, supplemented with appropriate antibiotics (tetracycline, kanamycin, and spectinomycin at 2.5, 10, and 10 μg/ml, respectively), either chemoheterotrophically (Res growth conditions) or photoheterotrophically in anaerobic jars with H_2+CO_2-generating gas packs from BBL Microbiology Systems (Cockeysville, MD) (Ps growth conditions). Plus and minus signs indicate the ability of the strains to form visible colonies after approximately 3 days of incubation under appropriate growth conditions. *E. coli* strains were grown on Luria broth (LB) supplemented as needed with appropriate antibiotics (tetracycline, kanamycin, spectinomycin, and ampicillin at 12.5, 50, 50, and 100 μg/ml, respectively).

Preparation of enriched medium supplemented with redox-active chemicals or various nutritional compounds. To characterize the medium-dependent phenotype of the *ccmI* suppressors like MT-SRP1.r1, enriched medium plates were supplemented at the same final concentrations with different nutritional compounds that make up the minimal medium (57). These were 0.2% (wt/vol) sodium succinate (pH 6.8), 0.01% (wt/vol) glutamic acid (pH 7.0), 0.004% (wt/vol) aspartic acid (pH 7.0), 0.05% (wt/vol) ammonium sulfate, 20 mM potassium phosphate (pH 6.8), 0.05% (wt/vol) sodium chloride, 0.2% (vol/vol) solution C consisting of 0.02% (wt/vol) nitrilotriacetic acid, 8.6 μM EDTA, 2.39 mM $MgSO_4$, 0.45 mM $CaCl_2 \cdot H_2O$, various trace elements [$ZnSO_4 \cdot 7H_2O$, $FeSO_4 \cdot 7H_2O$, $MnSO_4 \cdot H_2O$, $CuSO_4 \cdot 5H_2O$, $Co(NO_3)_2 \cdot 6H_2O$, and H_3BO_3] as in minimal medium, and a vitamin cocktail containing 0.1 mg/ml nicotinic acid, 0.05 mg/ml thiamine-HCl, and 1 μg/ml biotin. Enriched medium supplemented with various redox-active chemicals were prepared by adding cystine (0.05, 0.5, and 5 mM), diamide (*N,N,N′,N′*-tetramethylazodicarboxamide) (1, 10, and 100 μM), cysteine (0.1, 1, and 10 mM) and MESNA (2-mercaptoethanesulfonic acid) (0.1, 1, and 10 mM) or a mixture of cystine:cysteine at a 1:2 ratio (0.05:0.1, 0.5:1 and 5:10 mM) from appropriate fresh stock solutions. Plates were used immediately following solidification to determine the Res and Ps growth phenotypes of appropriate strains.

Molecular genetic techniques. Standard molecular genetic techniques were performed as described by Sambrook and Russell (52). Conjugal transfer of plasmids from *E. coli* to *R. capsulatus* was performed as described previously (12). The *R. capsulatus* strain MT-SRP1.r1big was grown under Ps conditions on enriched medium and its chromosomal DNA isolated by using the QIAGEN DNeasy kit (Valencia, CA). A genomic library was prepared as described previously (16, 17) by digesting chromosomal DNA with EcoRI and cloning the resulting fragments into the broad-host-range vector pRK415 (19). A 280-bp PCR product containing *ccmD* was amplified by using the primers helD-Fwd (5′-GCT CTA GAA CCG AGA TCC GCG CCC GTC G-3′) and helD-Rev (5′-GGG GTA CCC CCG CGC CAA CAA AGC CCG C-3′) carrying the recognition sites for the restriction enzymes XbaI and KpnI at their 5′ ends and was then cloned into the respective sites of pRK415 and pCHB500 to yield pCS1526 and pCS1527, respectively. Similarly, pCS1530 was constructed by PCR amplification of an 830-bp fragment containing *ccmC* using the primers helC2 (5′-CTT ATT CTA GAT TGA TGC GAG TC-3′) and helC3 (5′-GAC GCA AGG TAC CTG ACG GCG TAT TTT C-3′); pCS1531 was constructed by PCR amplification of a 1,010-bp fragment containing *ccmCD* using the primers helC2 and helD-Rev; pCS1532 was constructed by PCR amplification of a 1,490-bp fragment containing *ccmCDG* using the primers helC2 and RchelX1 (5′-GGC CCC GGT ACC AAG ACG CAG GAT-3′); and pCS1538 was constructed by PCR amplification of a 960-bp fragment containing *ubiE*::*ccmC* using the primers helC1 (5′-GAC AGT TCT AGA TCG GCA AGG GCA G-3′) and helC3 following appropriate restriction digestion and ligation of the amplified DNA fragments into pRK415. For the construction of pCS1540 and pCS1541, a 570-bp PCR product containing *ccmG* was amplified by using the primers helXforward-XbaI (5′-CGG GTC TAG AAA GCC CAG GAA GAA CGG A-3′) and RchelX1, a 750-bp PCR product containing *ccmDG* was amplified by using the primers helD-Fwd and RchelX1, respectively, and a restriction digestion and ligation procedure similar to that mentioned above was carried out by using the broad-host-range vector pCHB500 (6). For all of these plasmids, MT-SRP1.r1big chromosomal DNA was used as a template. To create pCS1542, a spectinomycin resistance cassette (2.0 kb) from pHP45Ω-Spec (47) was inserted in reverse orientation into the unique BamHI site of pCS1532 located in *ccmC*. Plasmid pCS1539 was obtained by cutting pCS1530 at its unique BamHI site and blunting the ends with T4 DNA polymerase before ligation, resulting in a frameshift mutation in *ccmC*. For construction of pCS1545, both cysteine codons 75 and 78 of *ccmG* in pCS1540 were mutated to serine codons by using primers HelX-C78Ss (5′-CTT CTG GGC TTC CTG GAG CGC GCC CTG TCG-3′) and HelX-C78Sas (5′-ACC CGA CAG GGC GCG CTC CAG GAA GCC CAG-3′) following the instructions of the QuikChange XL site-directed mutagenesis kit from Stratagene (La Jolla, CA). All plasmids were verified by DNA sequence analyses using appropriate primers (see below).

DNA sequence analysis. Automated DNA sequencing with the Big-Dye terminator cycle sequencing kit (Applied Biosystems) was performed according to the manufacturer by using the helC2, helC3, M13-forward, and M13-reverse primers to verify all pRK415 and pCHB500 derivatives constructed in this study. Chromosomal DNA of MT1131, MT-SRP1.r1, and MT-SRP1.r1big isolated with the DNeasy kit were used as templates, and the ORF124/*ccmABCDG* promoter region was amplified using the primers RcORF124down (5′-CTG GCG CTG GTG CCG ATG CTG GAT C-3′) and RchelCpromup (5′-CGG CTC TCC TCC CTC TCG CGT CCC G-3′) to generate a 2,070-bp PCR product, which was purified by using the QIAGEN PCR purification kit and sequenced using the same primers. Similarly, the 5′ region of *ccmC* including the intergenic space between *ccmB* and *ccmC* was amplified by using the same DNA template and the primers helC2 and helC3 to yield an 830-bp PCR fragment, which was purified and sequenced by using the primer helC2. DNA sequence analyses, homology searches, and genome sequence comparisons were done using MacVector (Kodak) and BLAST software packages (3).

Biochemical techniques. Intracytoplasmic membrane vesicles, or chromatophores, were prepared in 20 mM MOPS (morpholinepropanesulfonic acid)-KOH buffer (pH 7.0) containing 1 mM KCl, 10 mM EDTA and a protease inhibitor cocktail (Complete, EDTA-free from Roche Inc., Indianapolis, IN) as recommended by the manufacturer using a French pressure cell (28). Protein concentrations were determined according to the method of Bradford (9) using the stain solution Bio-Safe Coomassie from Bio-Rad (Hercules, CA). Sodium dodecyl sulfate-polyacrylamide gel electrophoresis (SDS-PAGE) (16.5% T, 6% C) was used as described by Schaegger and von Jagow (53), and various *c*-type Cyts were revealed via their endogenous peroxidase activity using tetramethylbenzidine (TMBZ) and H_2O_2 (58). Cyt *c* oxidase activity of the colonies was detected using the Nadi reaction as described earlier (32). Antisera against CcmA and CcmG were produced, and immunoblot analyses were performed, as described elsewhere (26).

Chemicals. All chemicals were of reagent grade and obtained from commercial sources.

RESULTS

Suppressors of CcmI-null mutants that are Ps$^+$/Nadi$^+$ on both minimal and enriched media. *R. capsulatus* CcmI-null mutants, such as MT-SRP1, are Ps$^-$/Nadi$^-$ on both minimal and enriched media due to their inability to produce *c*-type holo-Cyts (38). Ps$^+$ revertants of MT-SRP1, such as MT-SRP1.r1, are readily isolated (at a frequency of approximately 10^{-6}) on minimal, but not enriched, medium. These revertants overexpress *ccmFH*$_{Rc}$ to bypass the need for CcmI during *c*-type Cyt biogenesis (16). However, they are Ps$^+$ only on minimal medium, indicating that in such strains *c*-type Cyt production becomes restricted under different growth conditions. Interestingly, they acquire extra mutations (at a frequency of about 10^{-6}) in addition to the overexpression of *ccmFH*$_{Rc}$ (such as MT-SRP1.r1big) to become Ps$^+$ on enriched medium (Table 2).

A conjugally transferable genomic library with EcoRI-digested chromosomal DNA from MT-SRP1.r1big was used to complement MT-SRP1.r1 for Ps$^+$ growth on enriched medium and yielded the plasmids pDA5 and pDA10 (Fig. 2). pDA5 contained two EcoRI inserts of 1.6 and 1.4 kb, whose DNA sequence comparisons to the *R. capsulatus* genome sequence (http://ergo.integratedgenomics.com) indicated that they are not contiguous on the chromosome. The 1.6-kb insert consisted of two incomplete open reading frames (ORFs) (RRC03382 and RRC03385, which corresponds to *ubiE* (ubiquinone-menaquinone biosynthesis methyltransferase) of *R. capsulatus*. The 1.4-kb insert carried a 588-bp 3′ fragment of

TABLE 1. Bacterial strains and plasmids used in this study

Strain or plasmid	Description	Relevant phenotype[b]	Source or reference
Strains			
E. coli HB101	F$^-$ Δ(*gpt-proA*)*62 araC14 leuB6*(Am) *glnV44*(AS) *galK2*(Oc) *lacY1* Δ(*mcrC-mrr*) *rpsL20*(Str^r) *xylA5 mtl-1 thi-1*	Str^r	52
R. capsulatus			
SB1003[a]		Wild type; Res$^+$/Nadi$^+$ Ps$^+$ Cyt *c*$^+$	64
MT1131[a]	*crtD121* Rif^r	Wild type; Res$^+$/Nadi$^+$ Ps$^+$ Cyt *c*$^+$	55
Y262		GTA overproducer	63
MT-SRP1	Δ(*ccmI*::*kan*)	Res$^+$/Nadi$^-$ Ps$^-$; Cyt *c*$^-$	38
MT-SRP1.r1	Δ(*ccmI*::*kan*) G488A in promoter of $ccmFH_{Rc}$	Res$^+$/Nadi$^+$ Ps$^+$ Cyt *c*$^+$ on MedA	16
MT-SRP1.r1big	Δ(*ccmI*::*kan*) G488A in promoter of $ccmFH_{Rc}$ unknown mutation	Res$^+$/Nadi$^+$ Ps$^+$ Cyt *c*$^+$ on MedA and MPYE	16
SB1003Δ*helD*	Δ(*ccmD*::*kan*)	Res$^+$/Nadi$^-$ Ps$^-$ Cyt *c*$^-$	26
SB1003Δ*helX*	Δ(*ccmG*::*kan*)	Res$^+$/Nadi$^-$ Ps$^-$ Cyt *c*$^-$	4
TCK2	Δ(*pyrE*::*kan*), Δ(*ccmC*::*pyrE*)	Res$^+$/Nadi$^-$ Ps$^-$	62
KR319	Δ(*ccmA*::*kan*)	Res$^+$/Nadi$^-$ Ps$^-$ Cyt *c*$^-$	5
MD12	*ccmF*::*spe* ($ccmH_{Rc}^+$)	Res$^+$/Nadi$^-$ Ps$^-$ Cyts *c*$^-$	16
MD14	(*ccmF*$^+$) $ccmH_{Rc}$::*spe*	Res$^+$/Nadi$^-$ Ps$^-$ Cyt *c*$^-$	16
Plasmids			
pBluescript II SK(+)		Amp^r	Stratagene
pHP45Ω-Spec		Spe^r	47
pRK2013		Kan^r, helper	19
pRK404	Broad host-range vectors, gene expression could be supported by *E. coli lacZ* promoter	Tet^r	19, 31, 36
pRK415			
pUCA9			
pCHB500	Broad host-range expression vector via *R. capsulatus cycA* promoter	Tet^r	6
pDA5	pRK415 derivative with 1.6- and 1.4-kb chromosomal EcoRI fragments from MT-SRP1.r1big	Tet^r	This work
pDA10	pRK415 derivative with 3.1-kb and 13.5-kb chromosomal EcoRI fragments from MT-SRP1.r1big	Tet^r	This work
p2hel-404	pRK404 derivative with *ccmABCDG*	Amp^r Tet^r	38
pCS1526	280-bp PCR product containing *ccmD* from MT-SRP1.r1big cloned into XbaI-KpnI sites of pRK415	Tet^r	This work
pCS1527	280-bp PCR product containing *ccmD* from MT-SRP1.r1big cloned into XbaI-KpnI sites of pCHB500	Tet^r	This work
pCS1530	830-bp PCR product containing *ccmC* from MT-SRP1.r1big cloned into XbaI-KpnI sites of pRK415	Tet^r	This work
pCS1531	1.01-kb PCR product containing *ccmCD* from MT-SRP1.r1big cloned into XbaI and KpnI sites of pRK415	Tet^r	This work
pCS1532	1.49-kb PCR product containing *ccmCDG* from MT-SRP1.r1big cloned into XbaI and KpnI sites of pRK415	Tet^r	This work
pCS1534	1.4-kb EcoRI fragment of pDA5 cloned into pRK415	Tet^r	This work
pCS1535	1.6-kb EcoRI fragment of pDA5 cloned into pRK415	Tet^r	This work
pCS1536	3.1-kb EcoRI fragment from pDA10 in pRK415	Tet^r	This work
pCS1537	13.5-kb EcoRI fragment from pDA10 in pRK415	Tet^r	This work
pCS1538	960-bp PCR product containing *ubiE*::*ccmC* from pDA5 cloned in XbaI-KpnI sites of pRK415	Tet^r	This work
pCS1539	Δ*ccmC* created by filling the unique BamHI site of pCS1532	Tet^r	This work
pCS1540	570-bp PCR product containing *ccmG* from MT-SRP1.r1big cloned into XbaI-KpnI sites of pCHB500	Tet^r	This work
pCS1541	750-bp PCR product containing *ccmDG* from MT-SRP1.r1big cloned into XbaI-KpnI sites of pCHB500	Tet^r	This work
pCS1542	Spe^r cassette from pHP45Ω cloned into the BamHI site of *ccmC* gene in pCS1532	Tet^r Spe^r	This work
pCS1545	Replacement of *ccmG* cysteines 75 and 78 with serines in pCS1540	Tet^r	This work
pMM401	7-kb fragment containing G488A promoter-up allele of $ccmFH_{Rc}$ in pRK404	Tet^r	16
pMM403	7-kb fragment containing G488 wild-type promoter allele of $ccmFH_{Rc}$ in pRK404	Tet^r	16

Continued on following page

TABLE 1—*Continued*

Strain or plasmid	Description	Relevant phenotype[b]	Source or reference
pMM500	pMM401 derivative with a frameshift mutation in *ccmF*	Tet^r, $CcmF^-$ $CcmH_{Rc}{}^+$	16
	pYZ10 derivative with a nonpolar Spe^r cassette cloned into *ccmF*	Tet^r Spe^r $CcmF^-$ $CcmH_{Rc}{}^+$	
pYZ4			16
pYZ10	2.8-kb fragment containing G488A promoter-up allele of $ccmFH_{Rc}$ in pRK404	Tet^r	16
pYZ12	pYZ10 derivative with a nonpolar Spe^r cassette cloned into $ccmH_{Rc}$	Tet^r Spe^r, $CcmF^+$ $CcmH_{Rc}{}^-$	16
pK1	*ccdA* in pRK404	Tet^r	15
pMD1	*ccmE* in pRK404	Tet^r	15

[a] *R. capsulatus* SB1003 and MT1131 are both referred to as wild-type strains with respect to their Cyt *c* profile and growth properties. Y262, SB1003Δ*helD*, and SB1003Δ*helX* are derivatives of SB1003, and all other listed *R. capsulatus* strains are derivatives of MT1131.
[b] MedA and MPYE refer to minimal and enriched growth media, respectively.

ccmC (RRC02437), the *ccmDG* (RRC02436) portion of the ORF124/*ccmABCDG* operon involved in Cyt *c* biogenesis (5), and an additional incomplete ORF (RRC02435). Similarly, pDA10 also contained two noncontiguous chromosomal inserts (3.1 and 13.5 kb). The 3.1-kb fragment consisted of one complete (RRC04065) and two incomplete (RRC04064 and RRC02911) ORFs (Fig. 2). On the other hand, the 13.5-kb fragment carried seven complete (RRC00283 through RRC00285, RRC00288 through RRC00290, and RRC02361) and three incomplete (RRC00282 and overlapping RRC00291 and RRC04574) ORFs, as well as the $ccmFH_{Rc}$ gene cluster (RRC00286 and RRC00287), which is required for Cyt *c* maturation (5).

Hyperexpression of $ccmFH_{Rc}$ can render MT-SRP1.r1 Ps^+ on enriched medium. The plasmid pDA10 was analyzed by cloning its two EcoRI inserts separately into pRK415 to yield pCS1536 and pCS1537, respectively (Table 2). Of these plasmids, pCS1537 complemented MT-SRP1.r1 for Ps^+ growth on enriched medium, whereas pCS1536 did not, indicating that the complementing activity was associated with the large EcoRI insert containing the $ccmFH_{Rc}$ gene cluster (Fig. 2). As this fragment was originated from MT-SRP1.r1big, which is a derivative of MT-SRP1.r1 comprising a chromosomal overexpressing allele of $ccmFH_{Rc}$ (16), cells harboring pDA10 were considered to hyperexpress $ccmFH_{Rc}$ due to an increased copy number of these genes. Consistent with this assumption, it was observed that, while the plasmids pMM401 and pYZ10, which contain an overexpressing allele of $ccmFH_{Rc}$ mediated the Ps^+ growth of MT-SRP1.r1 on enriched medium, pMM403, which carries a wild-type allele of $ccmFH_{Rc}$, or pYZ4 and pYZ12, which are $CcmF^-$ $CcmH_{Rc}{}^+$ and $CcmF^+$ $CcmH_{Rc}{}^-$ derivatives of pYZ10, could not do so (Fig. 3). As both pYZ4 and pYZ12 complemented appropriate $CcmF^-$ and $CcmH_{Rc}{}^-$ mutants (16), these results indicated that not only hyperexpression of $ccmFH_{Rc}$ but also intact *ccmF* and $ccmH_{Rc}$ were required for the Ps^+ phenotype of MT-SRP1.r1 on enriched medium.

TABLE 2. Phenotypes of various CcmI-null mutants and their derivatives

Strain	Relevant characteristics	Phenotype on[a]:			
		MedA		MPYE	
		Res/ Nadi	Ps	Res/ Nadi	Ps
MT1131	$CcmI^+$ $CcmF^+$ $CcmH_{Rc}{}^+$	+/+	+	+/+	+
MT-SRP1	$CcmI^-$ $CcmF^+$ $CcmH_{Rc}{}^+$	+/−	−	+/−	−
MT-SRP1.r1	$CcmI^-$ $CcmF^{up}$ $CcmH_{Rc}{}^{up}$	+/+	+ (slow)	+/+	−
MT-SRP1.r1big	$CcmI^-$ $CcmF^{up}$ $CcmH_{Rc}{}^{up}$ BigX[b]	+/+	+	+/+	+

[a] MedA and MPYE refer to minimal and enriched growth media, respectively. For Res and Ps, + and − refer to the ability of the strains to grow under these conditions. For Nadi, + and − indicate the presence or absence of the Cyt *c* oxidase activity, respectively.
[b] BigX refers to the unknown mutated allele that confers the $Nadi^+/Ps^+$ phenotype to MT-SRP1.r1 on enriched medium.

Chromatophore membranes and soluble fractions prepared from appropriate MT-SRP1.r1 ($CcmI^-$ $CcmFH_{Rc}{}^{up}$) derivatives grown by Res in enriched medium were analyzed by TMBZ SDS-PAGE to confirm that overproduction of $CcmFH_{Rc}$ correlated with increased production of *c*-type Cyts. The amounts of membrane-bound (Fig. 4) and soluble (data not shown) *c*-type Cyts present in derivatives of MT-SRP1.r1 containing pDA10 and pYZ10 (both $ccmFH_{Rc}{}^{up}$) were higher than in those carrying pYZ4 (*ccmF*::*spe* $ccmH_{Rc}$) and pYZ12 (*ccmF* $ccmH_{Rc}$::*spe*), although still lower than in the wild-type strain MT1131. Therefore, whereas overexpression of $ccmFH_{Rc}$ was sufficient to overcome the Ps^- phenotype of a CcmI-null mutant on minimal medium, its additional hyperexpression via plasmid-borne copies was required for Ps^+ growth on both media.

Multiple copies of *ccmCDG* can mediate Ps growth of MT-SRP1.r1 on enriched medium. The two EcoRI inserts of pDA5 were also cloned separately into the conjugally transferable plasmid pRK415 to yield pCS1534 and pCS1535 (Fig. 5; Table 1). However, neither of these plasmids complemented MT-SRP1.r1 for Ps^+ growth on enriched medium, even though both pCS1534 and pDA5 did so for CcmD-null (SB1003 Δ*helD*) and CcmG-null (SB1003 Δ*helX*) mutants (Fig. 5). This finding suggested that, although the 1.4-kb fragment (pCS1534) contained expressed wild-type copies of *ccmD* and *ccmG*, including a truncated form of *ccmC* (′*ccmC*), both of the EcoRI inserts were required for complementation of MT-SRP1.r1 by pDA5. On the other hand, the plasmids p2hel-404 containing *ccmABCDG* and pCS1532 carrying *ccmCDG* clusters conferred Ps^+ growth ability on MT-SRP1.r1 on enriched medium like pDA5 (Fig. 5, rows 4 and 5). Thus, providing

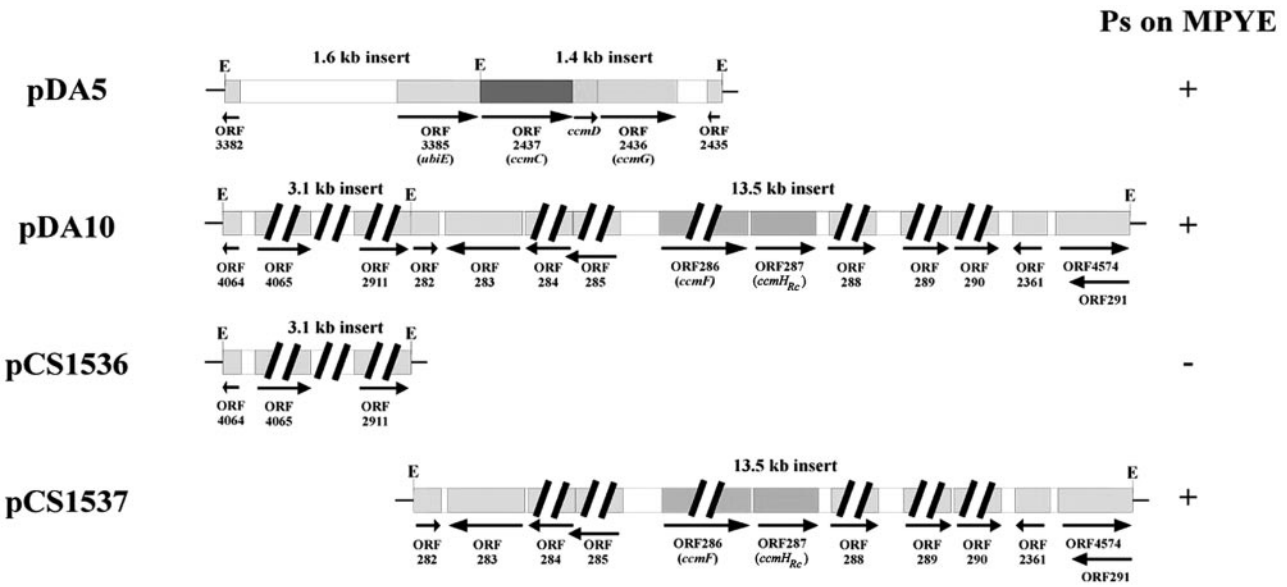

FIG. 2. Plasmids pDA5 and pDA10, which confer the Ps^+ growth phenotype on MT-SRP1.r1. The 1.4- and 1.6-kb EcoRI fragments of pDA5 are not contiguous with each other on the *R. capsulatus* chromosome. The 1.4-kb fragment carries two complete (*ccmD* and RRC02436 [*ccmG*]) and two incomplete (RRC02435 [*hpt*, hypoxanthine-guanine phosphoribosyltransferase] and RRC02437 [*ccmC*]) ORFs. The 1.6-kb fragment contains two incomplete ORFs, RRC03382 (*ysiB*, putative enoyl-CoA hydratase) and RRC03385 (*ubiE*, ubiquinone/menaquinone biosynthesis methyltransferase). The two EcoRI fragments of pDA10 are also noncontiguous on the *R. capsulatus* chromosome. The 3.1-kb fragment carries one complete (RRC04065 [*serC*]) and two incomplete (RRC04064 [*serB*] and RRC02911 [*serA*]) ORFs involved in serine biosynthesis. The 13.5-kb fragment contains nine complete ORFs (RRC00283 [*entB*, isochorismatase], RRC00284 and RRC00285 [*argF* and *argD*, respectively, involved in arginine biosynthesis], RRC00286 and RRC00287 [*ccmF* and *ccmH*$_{Rc}$, respectively, encoding the putative apo-Cyt *c* heme ligation complex CcmF and CcmH$_{Rc}$], RRC00288 [*fadB*, enoyl-CoA hydratase], RRC00289 [*msbA*, ATP binding lipid transporter], RRC00290 [*acs*, acetyl-CoA synthetase], and RRC002361 [*cspA*, cold shock DNA binding protein]), and three incomplete (RRC00282 [*hrpB*, ATP-dependent helicase], and overlapping RRC00291 [*miaB*, 2-methylthioadenine synthetase] and RRC04574 [a putative membrane protein with a possible oxidoreductase function]). The ability of pDA5, pDA10, pCS1536, and pCS1537 to confer on MT-SRP1.r1 a Ps^+ phenotype on enriched medium is indicated to the right, E refers to EcoRI cleavage sites, and thick slashes indicate that the ORFs and the intergenic spaces are truncated as needed to fit the figure.

multiple copies of *ccmCDG* in *trans* was sufficient to render MT-SRP1.r1 Ps^+ on enriched medium.

Chromatophore membrane and supernatant fractions prepared from various MT-SRP1.r1 ($CcmI^-$ $CcmFH_{Rc}{}^{up}$) derivatives grown by respiration in enriched medium were analyzed by TMBZ SDS-PAGE to correlate the growth phenotypes monitored here with the Cyt *c* profile changes. These analyses confirmed that the amounts of the membrane-bound Cyts c_p, c_1, c_y, and c_o in MT-SRP1.r1big and MT-SRP1.r1 derivatives harboring p2hel-404 (*ccmABCDG*), pCS1532 (*ccmCDG*), and pDA5 (*ubiE*::*ccmC ccmDG*) (Fig, 6A, lanes 3 to 6) were similar to those seen in the wild-type strain MT1131 (Fig. 6A, lane 1), whereas those in MT-SRP1.r1 and its derivative containing pCS1534 (′*ccmC ccmDG*) were lower (Fig. 6A, lanes 2 and 7), which is in agreement with their respective Ps phenotypes. Likewise, the amounts of Cyt c_2 and c' in MT-SRP1.r1big and MT-SRP1.r1 derivatives carrying p2hel-404, pCS1532 and pDA5 were also similar to those in wild-type samples (Fig. 6B, lanes 3 to 6) but again lower in MT-SRP1.r1 and its derivative harboring pCS1534 (Fig. 6B, lanes 2 and 7). Thus, the Ps^+ phenotypes on enriched medium accompanied increased steady-state amounts of various *c*-type Cyts.

A promoter upstream of *ccmC* is responsible for Ps^+ growth of MT-SRP1.r1 on enriched medium. In order to understand how pDA5, which contained only a truncated form of *ccmC*, could still complement MT-SRP1.r1, the junction region spanning its two EcoRI fragments was examined. In pDA5, the 507-bp 5′ end of *ubiE* including a sequence that resembles a *R. capsulatus* promoter in correct orientation with respect to *ccmDG* carried by the 1.6-kb insert was fused in frame to the 588-bp 3′ end of *ccmC* located on the 1.4-kb insert. Thus, this fortuitous construction either created a functional *ubiE*::*ccmC* fusion product or provided an additional promoter, thereby increasing the expression of the downstream genes *ccmD* and *ccmG*. The first possibility was excluded, because pDA5, unlike pCS1532 or p2hel-404 carrying an intact *ccmC*, could not complement a nonpolar CcmC-null mutant like TCK2 (62) (Fig. 5, rows 1 to 5). In addition, neither pCS1530 carrying an intact *ccmC* nor pCS1538 containing the *ubiE*::*ccmC* fusion could mediate Ps^+ growth of MT-SRP1.r1 on enriched medium (Table 1 and data not shown). On the other hand, the second possibility, that a promoter is located upstream of *ccmC*, was supported by the fact that pCS1539 carrying a frameshift mutation in *ccmC* (*ccm*Δ*C*) but not pCS1542 containing a polar *ccmC*::*spe* insertion (47) was able to restore the Ps^+ phenotype of MT-SRP1.r1 on enriched medium (Table 1). Indeed, control experiments indicated that both pCS1539 and pCS1542 complemented appropriate $CcmD^-$ (SB1003 Δ*ccmD*) and $CcmG^-$ (SB1003 Δ*ccmG*) mutants to $Ps^+/Nadi^+$ (Fig. 5, rows 6 and 7). Thus, it was concluded that the complementation seen with pDA5 was due to the *ubiE* promoter.

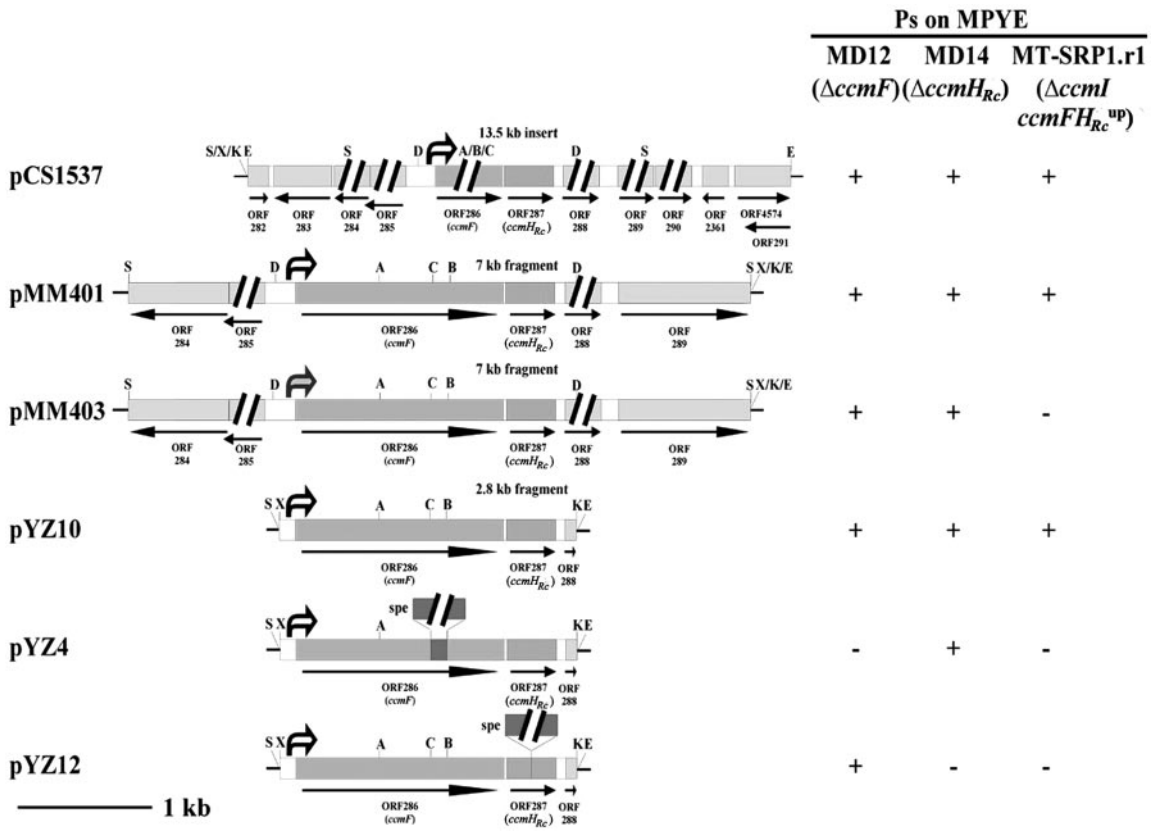

FIG. 3. Comparison of plasmids carrying various alleles of *ccmF-ccmH*$_{Rc}$. Plasmids pCS1537, pMM401, and pYZ10 carry a *ccmF-ccmH*$_{Rc}$ up-promoter allele, whereas pMM403 has a wild-type *ccmF-ccmH*$_{Rc}$ allele (Table 1). Plasmids pYZ4 and pYZ12 are CcmF$^-$ CcmH$_{Rc}$$^+$ and CcmF$^+$ CcmH$_{Rc}$$^-$ derivatives, respectively, of pYZ10. The ability of various plasmids to complement null mutants of CcmF (MD12), CcmH$_{Rc}$ (MD14), and CcmI (MT-SRP1.r1) for Ps$^+$ growth on enriched medium is indicated to the right. White arrows with black borders and the gray arrow refer to the promoter-up allele and wild type of *ccmF-ccmH*$_{Rc}$, respectively, and S, X, K, E, D, A, B, and C refer to cleavage sites of the restriction enzymes SphI, XbaI, KpnI, EcoRI, BclI, SacI, BamHI, and ClaI, respectively.

Overproduction of *ccmG* is sufficient for Ps$^+$ growth of MT-SRP1.r1 on enriched medium. The plasmids pCS1527, pCS1540, and pCS1541, overexpressing *ccmD*, *ccmG*, and *ccmDG*, respectively, via the *R. capsulatus cycA* promoter, were constructed to probe whether Ps$^+$ growth of MT-SRP1.r1 on enriched medium (Table 1) required either or both of these genes. Upon conjugation into MT-SRP1.r1, both pCS1540 and pCS1541, but not pCS1527, were able to confer Ps$^+$ growth on enriched medium, indicating that overexpression of only *ccmG* was sufficient for this phenotype (Fig. 5, rows 8 to 10). Appropriate MT-SRP1.r1 (CcmI$^-$ CcmFH$_{Rc}$^{up}) derivatives were then subjected to immunoblot analyses using polyclonal antibodies against CcmG to confirm that overexpression of *ccmG* via additional *ccmABCDG*-endogenous or -exogenous promoters resulted in its overproduction. The amounts of the 18-kDa CcmG protein (41) were indeed higher in the Ps$^+$ derivatives of MT-SRP1.r1 containing pCS1541 (*ccmDG*), pCS1540 (*ccmG*) and pCS1539 (*ccmΔC* and *ccmDG*) and thus overexpressing *ccmG* via an additional promoter than in the Ps$^-$ derivatives of the same strain carrying pCS1527 (*ccmG*) and pCS1542 (*ccmC*::*spe* and *ccmDG*) (Fig. 7A, compare lanes 3, 5, and 7 to 4 and 6). Equally, in chromatophore membranes of MT-SRP1.r1 derivatives carrying p2hel404 (*ccmABCDG*), pCS1532 (*ccmCDG*) and pDA5 (*ubiE*::*ccmC* and *ccmDG*)

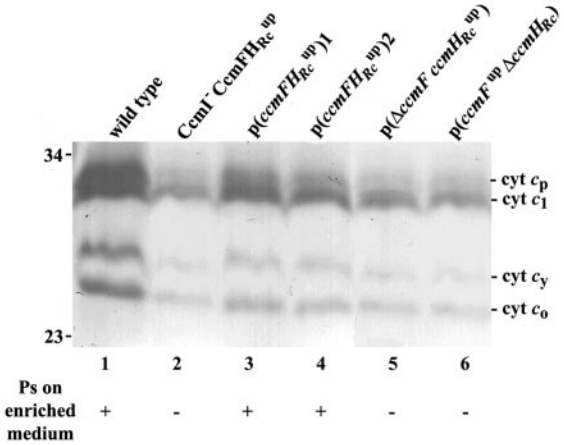

FIG. 4. *c*-type Cyt profiles of various pDA10-related Ps$^+$ derivatives of MT-SRP1.r1. Chromatophore membranes were prepared from *R. capsulatus* strains grown in enriched medium under respiratory condition and subjected to TMBZ SDS-PAGE analyses as described in Materials and Methods. Approximately 75 μg of proteins of strains MT1131 (wild type), MT-SRP1.r1 (CcmI$^-$ CcmFH$_{Rc}$^{up}), and its derivatives containing pDA10 [p(*ccmFH*$_{Rc}$^{up})1], pYZ10 [p(*ccmFH*$_{Rc}$^{up})], pYZ4 [p(Δ*ccmF ccmH*$_{Rc}$^{up})], and pYZ12 [p(*ccmF*^{up} Δ*ccmH*$_{Rc}$)], were loaded in each lane. Their respective Ps growth phenotypes on enriched medium are indicated at the bottom of the figure, and the molecular weight markers (in thousands) are shown on the left.

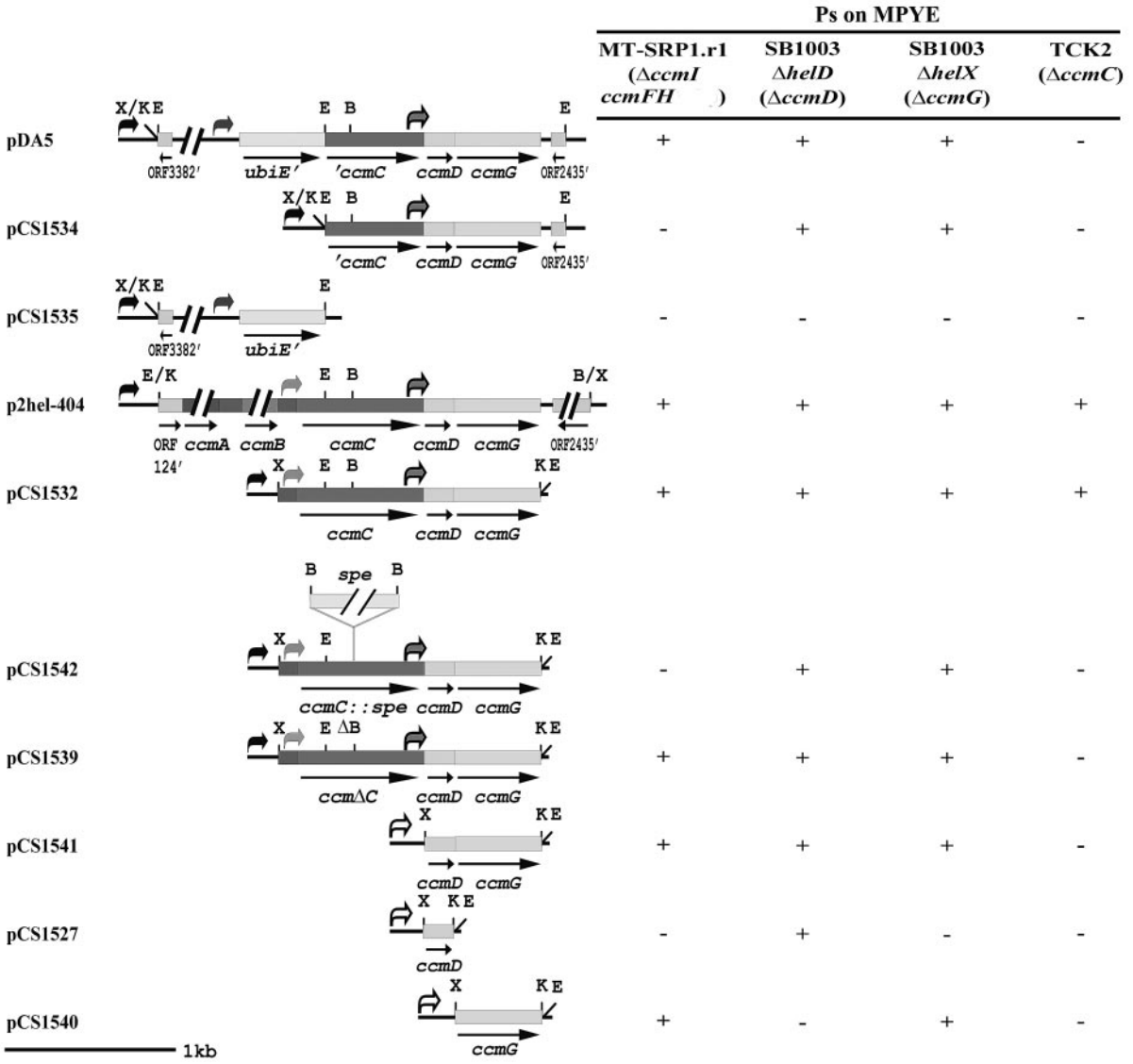

FIG. 5. Restriction maps of pDA5 and its derivatives. Plasmid pDA5 carries a *ubiE*::*ccmC* fusion in frame spanning the internal EcoRI site joining the 1.6- and 1.4-kb fragments, which are cloned separately to yield pCS1534 and pCS1535, respectively. Plasmids p2hel-404 and pCS1532 carry *ccmABCDG* and *ccmCDG*, respectively. pCS1542 and pCS1539 are derivatives of pCS1532 with a *ccmC*::*spe* insertion polar on the downstream genes *ccmDG* and a frameshift mutation in *ccmC* (*ccm*Δ*CB*), respectively. pCS1541, pCS1527 and pCS1540 are derivatives of pCHB500 and express *ccmDG*, *ccmD* and *ccmG*, respectively, via the *cycA* promoter. The ability of these plasmids to complement the CcmI-null mutant MT-SRP1.r1, the CcmD-null mutant SB1003 Δ*helD*, the CcmG-null mutant SB1003 Δ*helX*, and the CcmC-null mutant TCK2 for Ps^+ growth on enriched medium is shown on the right. Curved arrows refer to various promoters mediating different levels of expression of downstream genes, as follows. Black arrow, *E. coli lacZ* promoter; dark gray arrow, *ubiE* promoter; light gray arrow, promoter downstream of the *ccmB* and upstream of the EcoRI site in *ccmC*; white arrow with black border, *cycA* promoter; gray arrow with black border, promoter downstream of the BamHI site in *ccmC* and upstream of *ccmD*). X, K, E, and B refer to cleavage sites of the restriction enzymes XbaI, KpnI, EcoRI, and BamHI, respectively.

CcmG amounts were higher than those in derivatives harboring pCS1534 (′*ccmC* and *ccmDG*) and the wild-type strain MT1131 (Fig. 7B, compare lanes 5 to 7 to 2 and 8), which in turn were higher than those in MT-SRP1.r1 and MT-SRP1.r1big (Fig. 7B, lanes 3 and 4). As a control, the 25-kDa membrane-associated protein CcmA (26) was absent in a CcmA-null mutant (KR319) and not overproduced in MT-SRP1.r1, MT-SRP1.r1big, or MT-SRP1.r1 derivatives carrying additional copies of various portions of the *ccmABCDG* cluster (i.e., p2hel404, pCS1532, pDA5, or pCS1534) (Fig. 7C). Thus, in all instances, the increased amounts of CcmG correlated with the Ps^+ phenotype of MT-SRP1.r1 derivatives, demonstrating that its overproduction in addition to that of CcmF and $CcmH_{Rc}$ resulted in restoration of sufficient Cyt *c* biogenesis in the absence of CcmI.

Profiles of *c*-type Cyts of MT-SRP1.r1 ($CcmI^-$ $CcmFH_{Rc}{}^{up}$) derivatives carrying various *ccmG* constructs were analyzed by TMBZ SDS-PAGE, using chromatophore membranes and sol-

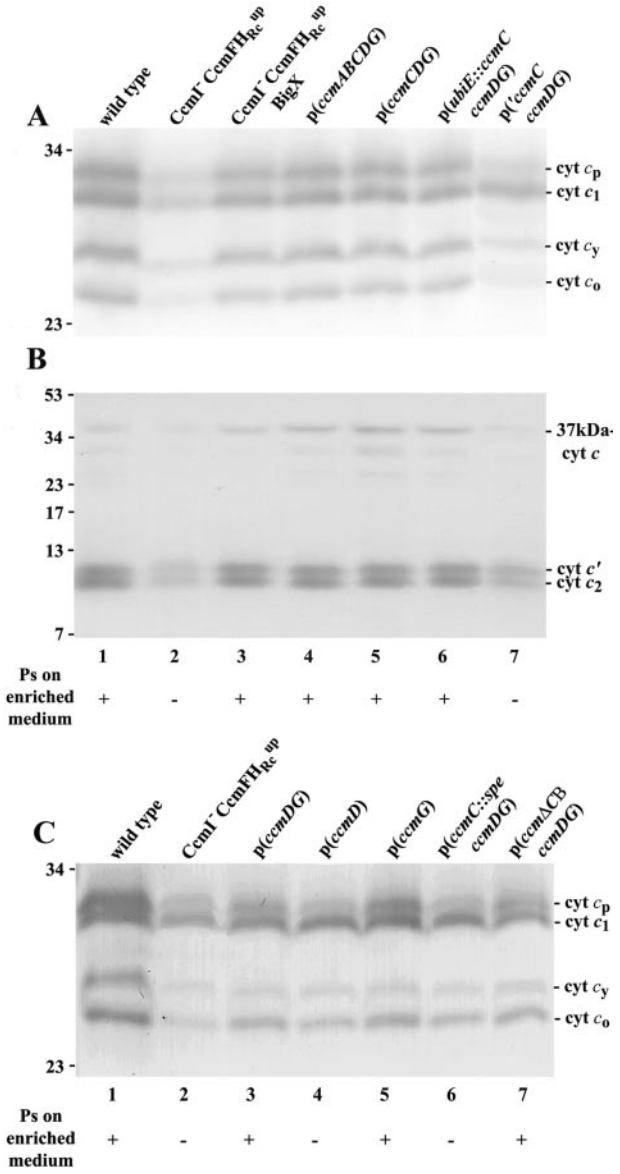

FIG. 6. *c*-type Cyt profiles of various pDA5-related Ps$^+$ derivatives of MT-SRP1.r1. Chromatophore membranes (A and C) and soluble fractions (B) prepared from *R. capsulatus* strains grown in enriched medium under respiratory conditions were subjected to TMBZ SDS-PAGE analyses, as described in Material and Methods. Approximately 75 μg of proteins was loaded in each lane, and the Ps growth phenotypes on enriched medium of the strains used are indicated at the bottom of the panels B and C. Panels A and B correspond to the membrane and soluble fractions, respectively, of MT1131 (wild type), MT-SRP1.r1 (CcmI$^-$ CcmFH$_{Rc}^{up}$), MT-SRP1.r1big (CcmI$^-$ CcmFH$_{Rc}^{up}$ BigX) and the MT-SRP1.r1 derivatives containing p2hel-404 [p(*ccmABCDG*)], pCS1532 [p(*ccmCDG*)], pDA5 [p(*ubiE*::*ccmCDG*)] and pCS1534 [p(*'ccmC ccmDG*)], and panel C corresponds to the membrane fractions of MT1131 (wild type), MT-SRP1.r1 (CcmI$^-$ CcmFH$_{Rc}^{up}$) and its derivatives carrying pCS1541 [p(*ccmDG*)], pCS1527 [p(*ccmD*)], pCS1540 [p(*ccmG*)], pCS1542 [p(*ccmC*::*spe ccmDG*)], and pCS1539 [p(*ccm*Δ*C*B *ccmDG*)], as listed in Table 1. The molecular weight markers (in thousands) are indicated on the left.

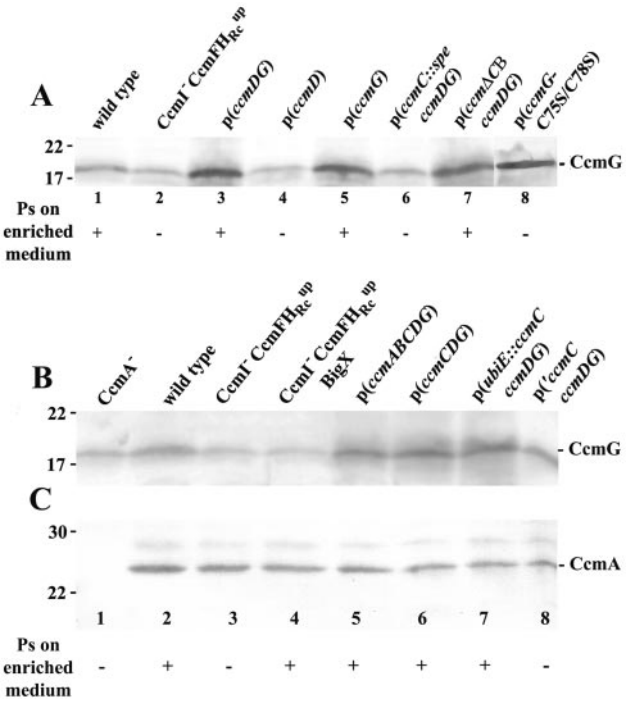

FIG. 7. Immunoblot analyses of CcmG and CcmA in MT-SRP1.r1 and its Ps$^+$ derivatives. Chromatophore membranes were prepared from *R. capsulatus* strains grown in enriched medium under respiratory conditions and subjected to SDS-PAGE, approximately 25 μg of protein was loaded in each lane, and immunoblot analyses using polyclonal antibodies against CcmG (A and B) and CcmA (C) were performed as described in Material and Methods. Strains KR319 (CcmA$^-$), MT1131 (wild type), MT-SRP1.r1 (CcmI$^-$ CcmFH$_{Rc}^{up}$), and MT-SRP1.r1big (CcmI$^-$ CcmFH$_{Rc}^{up}$ BigX) and the MT-SRP1.r1 derivatives harboring p2hel-404 [p(*ccmABCDG*)], pCS1532 [p(*ccmCDG*)], pDA5 [p(*ubiE*::*ccmCDG*)] and pCS1534 [p(*'ccmC ccmDG*)], pCS1541 [p(*ccmDG*)], pCS1527 [p(*ccmD*)], pCS1540 [p(*ccmG*)], pCS1542 [p(*ccmC*::*spe ccmDG*)], pCS1539 [p(*ccm*Δ*C*B *ccmDG*)] and pCS1545 [p(*ccmG*-C75S/C78S)] were used. Their respective Ps growth phenotypes on enriched medium are indicated at the bottom of panels A and C. Relevant molecular weight markers (in thousands) are also indicated.

uble fractions from cells grown under Res conditions in enriched medium. In agreement with the overproduction of CcmG, the amounts of membrane-bound (Fig. 6C) and soluble (data not shown) *c*-type Cyts were larger in the Ps$^+$ derivatives of MT-SRP1.r1 carrying pCS1541 (*ccmDG*), pCS1540 (*ccmG*) and pCS1539 (*ccm*Δ*C* and *ccmDG*) (lanes 3, 5 and 7) than in those containing pCS1527 (*ccmD*) and pCS1542 (*ccmC*::*spe* and *ccmDG*) (lanes 2, 4, and 6). However, they were still lower than those in the wild-type strain MT1131 (lane 1).

To further probe whether the thioredoxin function of CcmG was indeed required for its ability to confer Ps$^+$ growth on MT-SRP1.r1 in minimal and enriched media, its cysteine residues (Cys 75 and Cys 78) were replaced with serines in pCS1540 to yield pCS1545. This cysteineless CcmG derivative (CcmG-C75S/C78S) was unable to support Ps$^+$ growth of MT-SRP1.r1 on enriched media, although it was produced at adequate amounts (Fig. 7A, compare lanes 5 and 8). Thus, the thioredoxin motif of CcmG was necessary for its suppressor ability under the Ps growth conditions tested here.

DISCUSSION

In this work, a detailed analysis of the Ps^+ derivatives of CcmI-null suppressors that overproduce CcmF and $CcmH_{Rc}$ and that can grow on both minimal and enriched medium was undertaken to further define the role of CcmI in Cyt *c* biogenesis. Fortuitous isolation of a *ubiE*::*ccmCDG* fusion plasmid led to the discovery that overproduction of CcmG, a component involved in apo-Cyt *c* thioreduction, was sufficient to remedy the Ps growth inability on enriched medium of CcmI-null suppressors overproducing CcmF and $CcmH_{Rc}$. Overexpression of *ccmG* could be achieved via various promoter activities, presumably by increasing its transcription. Positioning *ccmG* either artificially downstream of the exogenous *ubiE* or *cycA* promoters or using chromosomal fragments carrying promoter activities that are naturally located upstream of it yielded appreciable overproduction of CcmG.

The data obtained also pointed out that the transcriptional organization of the *ccmABCDG* cluster is complex. In addition to a promoter located upstream of ORF124/*ccmA* (5), a second promoter located between the stop codon of *ccmB* and the EcoRI site within *ccmC* is also present as a plasmid harboring only *ccmCDG* (Table 1) could render MT-SRP1.r1 Ps^+ on enriched media. Moreover, since plasmids containing a polar insertion in *ccmC* or a fragment carrying a truncated *ccmC* upstream of intact *ccmD* and *ccmG* can complement appropriate $CcmD^-$ and $CcmG^-$ mutants as well (Fig. 5) but fail to support Ps^+ growth of MT-SRP1.r1 on enriched medium, a third, weaker promoter appears to be located downstream from the BamHI site in *ccmC* and upstream of *ccmD*. The presence of a promoter within the *ccmABCDG* cluster endowing *ccmCDG* with the ability to be expressed independently of *ccmAB* raises the possibility that the products of these two clusters could be synthesized in different stoichiometries.

In addition to CcmG overproduction, $CcmI^-$ mutants containing both chromosomal and plasmid-borne copies of a promoter-up allele of $ccmFH_{Rc}{}^{up}$ cluster (16), hence highly overproducing CcmF and $CcmH_{Rc}$ (data not shown), are also proficient for Cyt *c* maturation in minimal and enriched media. However, the photosynthetic growth of a $CcmI^-$ mutant carrying a chromosomal wild-type $ccmFH_{Rc}$ allele (e.g., MT-SRP1) is much slower (requiring at least 7 days of incubation) than growth of a mutant with a similar promoter-up $ccmFH_{Rc}{}^{up}$ allele (*e.g.*, MT-SRP1.r1). Furthermore, neither of these $CcmI^-$ mutants could be complemented for Ps^+ growth on enriched medium upon introduction of a plasmid-borne wild-type copy of the $ccmFH_{Rc}$ cluster (Fig. 3). Thus, a threshold level of CcmF and $CcmH_{Rc}$ overproduction appears to be required to overcome the absence of CcmI during Cyt *c* biogenesis.

The fact that both CcmG and $CcmH_{Rc}$ are known to be components of the thioreduction pathway (41), and that the thioredoxin motif of CcmG is required for suppression, raises the possibility that the growth defect of CcmI mutants on enriched medium might be due to a lack of adequate redox power to ensure sufficient holo-Cyt *c* formation. How the levels of CcmF, $CcmH_{Rc}$, and CcmG are regulated in *R. capsulatus* is not yet well known. Available data indicate that the amounts of $CcmH_{Rc}$ and possibly of CcmF are dramatically increased during Res, compared to Ps, growth conditions, whereas those of CcmG remain almost unchanged. Similarly, the levels of $CcmH_{Rc}$ and CcmG are higher in enriched than in minimal medium (24). These findings suggest that, while larger amounts of thioreduction components are required to support both Res and Ps growth in enriched medium, smaller amounts of CcmF and $CcmH_{Rc}$ are sufficient under Ps than under Res conditions. Although the amounts of CcmF, $CcmH_{Rc}$ and CcmG are regulated depending on the growth conditions, in the absence of CcmI, their levels might need to be adjusted to sustain productive Cyt *c* biogenesis. However, supplementation of enriched medium neither with different redox-active chemicals nor with the different nutritional constituents of the minimal medium (see Material and Methods) was sufficient to restore the Ps^+ phenotype of MT-SRP1.r1. Thus, bypassing the absence of CcmI might not be mediated solely by the increased protein dithiol:disulfide oxidoreductase activities via the overproduction of CcmG and $CcmH_{Rc}$.

Remarkably, suppression of *ccmI* always requires both CcmF and $CcmH_{Rc}$, as if these two components act together. In *E. coli*, CcmF, CcmE, and $CcmH_{Ec}$ coimmunoprecipitate, suggesting that they might form a heme ligation complex transferring heme from CcmE to apo-Cyt *c* (49). If a similar situation is also valid in *R. capsulatus* (16), then comparable interactions between CcmF, $CcmH_{Rc}$, CcmI, and CcmE might be expected (Fig. 1, bottom). Thus, a possibility is that overproduction of CcmG, CcmF, and $CcmH_{Rc}$ in the absence of CcmI might enhance more efficient interactions of the remaining components so that adequate thioreduction of, and heme ligation to, the apo-Cyt *c* substrates can occur. Alternatively, overproduction of CcmF and $CcmH_{Rc}$ could increase the capture rate of apo-Cyt *c* substrates by the heme ligation complex to compete out their proteolysis in the absence of specific protection factors like CcmI, as proposed earlier (16). In *E. coli*, the formation of specific disulfide intermediates between the thioredoxin motifs of CcmG and $CcmH_{Ec}$, respectively, as well as the heme binding motif of apo-Cyt *c* and the thioredoxin motif of $CcmH_{Ec}$, has been documented (23, 48). Conceivably, in the absence of CcmI, the rate of these interactions compared to that of apo-Cyt *c* proteolysis might be limiting.

Recently, it has been shown that expression in *trans* of the N-terminal transmembrane helix and the adjacent cytoplasmic loop of CcmI-1 is not sufficient for Cyt *c* maturation but alleviates the protoporphyrin IX (PPIX) accumulation phenotype of CcmI-null mutants in *Sinorhizobium meliloti* (10). This observation led to the proposal that in the absence of the CcmI-1 region, either heme synthesis via ferrochelatase or heme transport across the membrane is defective, leading to PPIX accumulation. However, the fact that CcmI-null mutants are fully proficient for *c*-type Cyt biogenesis by overproduction of CcmG in addition to CcmF and $CcmH_{Rc}$, as shown in this work, argues that the main function of CcmI might not be directly related to heme biosynthesis or delivery. It has been reported that CcmF in *Paracoccus denitrificans*, *Pseudomonas putida*, and *Rhizobium etli*, as well as CcmI in the latter species, is required not only for Cyt *c* maturation but also for siderophore synthesis and iron acquisition (18, 45, 65). In *R. etli*, $CcmF^-$ or $CcmI^-$ mutants also accumulate PPIX (65) raising the possibility that the CcmI-1 homologue of *S. meliloti* might be specifically involved in these periplasmic processes. Several *R. capsulatus* Cyt *c* biogenesis mutants exhibit a similar por-

phyrin excretion phenotype (7, 15, 26, 36); however, whether CcmI, CcmF and CcmH$_{Rc}$ are necessary for iron acquisition in this species remains to be seen.

How CcmI interacts with the *c*-type apo-Cyts is unknown. Disulfide bonds are thought to be formed within the cysteines of the conserved heme-binding motif of the apo-Cyt *c* (22), possibly via the DsbA and DsbB components of the periplasmic protein disulfide oxidoreductase pathway (39, 40, 50, 51). However, it is now clear that this thio-oxidative pathway is not essential for Cyt *c* maturation (1, 17, 20). Nonetheless, when it is present, these bonds may need to be reduced via the thioreduction branch prior to heme attachment (15, 30, 41). It is thus tempting to speculate that CcmI might interact with other Cyt *c* biogenesis components, such as CcmF, CcmH$_{Rc}$, and CcmG, via the leucine zipper-like domain in CcmI-1 (38), while recognizing the disulfide bond containing *c*-type apo-Cyt substrates via its tetratricopeptide-like (TPR) motifs in CcmI-2 (10) (Fig. 1), or vice versa. Whereas leucine zipper motifs facilitate dimerization (37, 42), TPR-containing proteins interact with a partner protein(s) in multiprotein complexes (8, 13).

Finally, it should be mentioned that overexpression of *ccmG* is not the molecular basis of the Ps$^+$ phenotype on enriched medium of the *ccmI* suppressor MT-SRP1.r1big (Table 2) (which was used to construct the initial chromosomal library), because similar amounts of CcmG are present in chromatophore membranes of MT-SRP1.r1 and MT-SRP1.r1big (Fig. 7B). Moreover, no DNA sequence difference in the 5′ upstream promoter region of the ORF124/*ccmABCDG* cluster or in the *ccmB-ccmC* intergenic region was found in MT-SRP1.r1big compared to MT-SRP1.r1 (data not shown). Thus, another mutation(s) in a currently unknown component(s), such as periplasmic proteases, might also confer Ps$^+$ growth ability on a CcmI-null mutant.

In summary, it is clear that overproduction of CcmG in addition to that of CcmF and CcmH$_{Rc}$ is necessary for full efficiency of Cyt *c* maturation in the absence of CcmI, suggesting specific interactions between these components. Future analyses of these interactions should provide further insights on the cross-point between the apo-Cyt *c* delivery and the thioreduction branches of Cyt *c* biogenesis.

ACKNOWLEDGMENTS

This work was supported by grants DOE 91ER20052 and NIH GM 38237 to F.D. and GM 47909 to R.G.K.

We thank K. Wade for her help during this work and J. W. Cooley for his editorial comments.

REFERENCES

1. **Allen, J. W., P. D. Barker, and S. J. Ferguson.** 2003. A cytochrome b_{562} variant with a *c*-type cytochrome CXXCH heme-binding motif as a probe of the *Escherichia coli* cytochrome *c* maturation system. J. Biol. Chem. **278:** 52075–52083.
2. **Allen, J. W., O. Daltrop, J. M. Stevens, and S. J. Ferguson.** 2003. *c*-type cytochromes: diverse structures and biogenesis systems pose evolutionary problems. Philos. Trans. R. Soc. Lond. B. **358:**255–266.
3. **Altschul, S. F., W. Gish, W. Miller, E. W. Myers, and D. J. Lipman.** 1990. Basic local alignment search tool. J. Mol. Biol. **215:**403–410.
4. **Beckman, D. L., and R. G. Kranz.** 1993. Cytochromes *c* biogenesis in a photosynthetic bacterium requires a periplasmic thioredoxin-like protein. Proc. Natl. Acad. Sci. USA **90:**2179–2183.
5. **Beckman, D. L., D. R. Trawick, and R. G. Kranz.** 1992. Bacterial cytochromes *c* biogenesis. Genes Dev. **6:**268–283.
6. **Benning, C., and C. R. Somerville.** 1992. Isolation and genetic complementation of a sulfolipid-deficient mutant of *Rhodobacter sphaeroides*. J. Bacteriol. **174:**2352–2360.
7. **Biel, S. W., and A. J. Biel.** 1990. Isolation of a *Rhodobacter capsulatus* mutant that lacks *c*-type cytochromes and excretes porphyrins. J. Bacteriol. **172:** 1321–1326.
8. **Blatch, G. L., and M. Lassle.** 1999. The tetratricopeptide repeat: a structural motif mediating protein-protein interactions. Bioessays **21:**932–939.
9. **Bradford, M. M.** 1976. A rapid and sensitive method for the quantitation of microgram quantities of protein utilizing the principle of protein-dye binding. Anal. Biochem. **72:**248–254.
10. **Cinege, G., A. Kereszt, S. Kertesz, G. Balogh, and I. Dusha.** 2004. The roles of different regions of the CycH protein in *c*-type cytochrome biogenesis in *Sinorhizobium meliloti*. Mol. Genet. Genomics **271:**171–179.
11. **Collet, J. F., and J. C. Bardwell.** 2002. Oxidative protein folding in bacteria. Mol. Microbiol. **44:**1–8.
12. **Daldal, F., S. Cheng, J. Applebaum, E. Davidson, and R. C. Prince.** 1986. Cytochrome c_2 is not essential for photosynthetic growth of *Rhodopseudomonas capsulata*. Proc. Natl. Acad. Sci. USA **83:**2012–2016.
13. **D'Andrea, L. D., and L. Regan.** 2003. TPR proteins: the versatile helix. Trends Biochem. Sci. **28:**655–662.
14. **Davidson, E., and F. Daldal.** 1987. Primary structure of the bc_1 complex of *Rhodopseudomonas capsulata.* Nucleotide sequence of the *pet* operon encoding the Rieske cytochrome *b*, and cytochrome c_1 apoproteins. J. Mol. Biol. **195:**13–24.
15. **Deshmukh, M., G. Brasseur, and F. Daldal.** 2000. Novel *Rhodobacter capsulatus* genes required for the biogenesis of various *c*-type cytochromes. Mol. Microbiol. **35:**123–138.
16. **Deshmukh, M., M. May, Y. Zhang, K. K. Gabbert, K. A. Karberg, R. G. Kranz, and F. Daldal.** 2002. Overexpression of *ccl1-2* can bypass the need for the putative apocytochrome chaperone CycH during the biogenesis of *c*-type cytochromes. Mol. Microbiol. **46:**1069–1080.
17. **Deshmukh, M., S. Turkarslan, D. Astor, M. Valkova-Valchanova, and F. Daldal.** 2003. The dithiol:disulfide oxidoreductases DsbA and DsbB of *Rhodobacter capsulatus* are not directly involved in cytochrome *c* biogenesis, but their inactivation restores the cytochrome *c* biogenesis defect of CcdA-null mutants. J. Bacteriol. **185:**3361–3372.
18. **de Vrind, J. P., G. J. Brouwers, P. L. Corstjens, J. den Dulk, and E. W. de Vrind-de Jong.** 1998. The cytochrome *c* maturation operon is involved in manganese oxidation in *Pseudomonas putida* GB-1. Appl. Environ. Microbiol. **64:**3556–3562.
19. **Ditta, G., T. Schmidhauser, E. Yakobson, P. Lu, X. W. Liang, D. R. Finlay, D. Guiney, and D. R. Helinski.** 1985. Plasmids related to the broad host range vector, pRK290, useful for gene cloning and for monitoring gene expression. Plasmid **13:**149–153.
20. **Erlendsson, L. S., and L. Hederstedt.** 2002. Mutations in the thiol-disulfide oxidoreductases BdbC and BdbD can suppress cytochrome *c* deficiency of CcdA-defective *Bacillus subtilis* cells. J. Bacteriol. **184:**1423–1429.
21. **Fabianek, R. A., H. Hennecke, and L. Thony-Meyer.** 1998. The active-site cysteines of the periplasmic thioredoxin-like protein CcmG of *Escherichia coli* are important but not essential for cytochrome *c* maturation in vivo. J. Bacteriol. **180:**1947–1950.
22. **Fabianek, R. A., H. Hennecke, and L. Thony-Meyer.** 2000. Periplasmic protein thiol:disulfide oxidoreductases of *Escherichia coli*. FEMS Microbiol. Rev. **24:**303–316.
23. **Fabianek, R. A., T. Hofer, and L. Thony-Meyer.** 1999. Characterization of the *Escherichia coli* CcmH protein reveals new insights into the redox pathway required for cytochrome *c* maturation. Arch. Microbiol. **171:**92–100.
24. **Gabbert, K. K., B. S. Goldman, and R. G. Kranz.** 1997. Differential levels of specific cytochrome *c* biogenesis proteins in response to oxygen: analysis of the *ccl* operon in *Rhodobacter capsulatus*. J. Bacteriol. **179:**5422–5428.
25. **Goldman, B. S., D. L. Beck, E. M. Monika, and R. G. Kranz.** 1998. Transmembrane heme delivery systems. Proc. Natl. Acad. Sci. USA **95:**5003–5008.
26. **Goldman, B. S., D. L. Beckman, A. Bali, E. M. Monika, K. K. Gabbert, and R. G. Kranz.** 1997. Molecular and immunological analysis of an ABC transporter complex required for cytochrome *c* biogenesis. J. Mol. Biol. **268:**724–738.
27. **Goldman, B. S., and R. G. Kranz.** 2001. ABC transporters associated with cytochrome *c* biogenesis. Res. Microbiol. **152:**323–329.
28. **Gray, K. A., M. Grooms, H. Myllykallio, C. Moomaw, C. Slaughter, and F. Daldal.** 1994. *Rhodobacter capsulatus* contains a novel *cb*-type cytochrome *c* oxidase without a CuA center. Biochemistry **33:**3120–3127.
29. **Kadokura, H., F. Katzen, and J. Beckwith.** 2003. Protein disulfide bond formation in prokaryotes. Annu. Rev. Biochem. **72:**111–135.
30. **Katzen, F., M. Deshmukh, F. Daldal, and J. Beckwith.** 2002. Evolutionary domain fusion expanded the substrate specificity of the transmembrane electron transporter DsbD. EMBO J. **21:**3960–3969.
31. **Keen, N. T., S. Tamaki, D. Kobayashi, and D. Trollinger.** 1988. Improved broad-host-range plasmids for DNA cloning in Gram-negative bacteria. Gene **70:**191–197.
32. **Keilin, D.** 1966. The history of cell respiration and cytochrome. Cambridge University Press, Cambridge, United Kingdom.
33. **Koch, H. G., O. Hwang, and F. Daldal.** 1998. Isolation and characterization of *Rhodobacter capsulatus* mutants affected in cytochrome cbb_3 oxidase activity. J. Bacteriol. **180:**969–978.

34. **Koch, H. G., H. Myllykallio, and F. Daldal.** 1998. Using genetics to explore cytochrome function and structure in *Rhodobacter*. Methods Enzymol. **297:** 81–94.
35. **Kranz, R., R. Lill, B. Goldman, G. Bonnard, and S. Merchant.** 1998. Molecular mechanisms of cytochrome *c* biogenesis: three distinct systems. Mol. Microbiol. **29:**383–396.
36. **Kranz, R. G.** 1989. Isolation of mutants and genes involved in cytochromes *c* biosynthesis in *Rhodobacter capsulatus*. J. Bacteriol. **171:**456–464.
37. **Landschulz, W. H., P. F. Johnson, and S. L. McKnight.** 1988. The leucine zipper: a hypothetical structure common to a new class of DNA binding proteins. Science **240:**1759–1764.
38. **Lang, S. E., F. E. Jenney, Jr., and F. Daldal.** 1996. *Rhodobacter capsulatus* CycH: a bipartite gene product with pleiotropic effects on the biogenesis of structurally different *c*-type cytochromes. J. Bacteriol. **178:**5279–5290.
39. **Metheringham, R., L. Griffiths, H. Crooke, S. Forsythe, and J. Cole.** 1995. An essential role for DsbA in cytochrome *c* synthesis and formate-dependent nitrite reduction by *Escherichia coli* K-12. Arch. Microbiol. **164:**301–307.
40. **Metheringham, R., K. L. Tyson, H. Crooke, D. Missiakas, S. Raina, and J. A. Cole.** 1996. Effects of mutations in genes for proteins involved in disulphide bond formation in the periplasm on the activities of anaerobically induced electron transfer chains in *Escherichia coli* K12. Mol. Gen. Genet. **253:**95–102.
41. **Monika, E. M., B. S. Goldman, D. L. Beckman, and R. G. Kranz.** 1997. A thioreduction pathway tethered to the membrane for periplasmic cytochromes *c* biogenesis; *in vitro* and *in vivo* studies. J. Mol. Biol. **271:**679–692.
42. **O'Shea, E. K., J. D. Klemm, P. S. Kim, and T. Alber.** 1991. X-ray structure of the GCN4 leucine zipper, a two-stranded, parallel coiled coil. Science **254:**539–544.
43. **Page, M. D., Y. Sambongi, and S. J. Ferguson.** 1998. Contrasting routes of *c*-type cytochrome assembly in mitochondria, chloroplasts and bacteria. Trends Biochem. Sci. **23:**103–108.
44. **Page, M. D., N. F. Saunders, and S. J. Ferguson.** 1997. Disruption of the *Pseudomonas aeruginosa dipZ* gene, encoding a putative protein-disulfide reductase, leads to partial pleiotropic deficiency in *c*-type cytochrome biogenesis. Microbiology **143:**3111–3122.
45. **Pearce, D. A., M. D. Page, H. A. Norris, E. J. Tomlinson, and S. J. Ferguson.** 1998. Identification of the contiguous *Paracoccus denitrificans ccmF* and *ccmH* genes: disruption of *ccmF*, encoding a putative transporter, results in formation of an unstable apocytochrome *c* and deficiency in siderophore production. Microbiology **144:**467–477.
46. **Pettigrew, G. W., and G. R. Moore.** 1987. Cytochromes *c.* Biological aspects. Springer Verlag, New York, N.Y.
47. **Prentki, P., and H. M. Krisch.** 1984. *In vitro* insertional mutagenesis with a selectable DNA fragment. Gene **29:**303–313.
48. **Reid, E., J. Cole, and D. J. Eaves.** 2001. The Escherichia coli CcmG protein fulfils a specific role in cytochrome *c* assembly. Biochem. J. **355:**51–58.
49. **Ren, Q., U. Ahuja, and L. Thony-Meyer.** 2002. A bacterial cytochrome *c* heme lyase. CcmF forms a complex with the heme chaperone CcmE and CcmH but not with apocytochrome *c*. J. Biol. Chem. **277:**7657–7663.
50. **Sambongi, Y., and S. J. Ferguson.** 1996. Mutants of *Escherichia coli* lacking disulphide oxidoreductases DsbA and DsbB cannot synthesise an exogenous monohaem *c*-type cytochrome except in the presence of disulphide compounds. FEBS Lett. **398:**265–268.
51. **Sambongi, Y., and S. J. Ferguson.** 1994. Specific thiol compounds complement deficiency in *c*-type cytochrome biogenesis in *Escherichia coli* carrying a mutation in a membrane-bound disulphide isomerase-like protein. FEBS Lett. **353:**235–238.
52. **Sambrook, J., and D. W. Russell.** 2001. Molecular cloning: a laboratory manual, 3rd ed. Cold Spring Harbor Laboratory Press, Cold Spring Harbor, N.Y.
53. **Schaegger, H., and G. von Jagow.** 1987. Tricine-sodium dodecyl sulfate-polyacrylamide gel electrophoresis for the separation of proteins in the range from 1–100 kDa. Anal. Biochem. **166:**368–379.
54. **Schulz, H., H. Hennecke, and L. Thony-Meyer.** 1998. Prototype of a heme chaperone essential for cytochrome *c* maturation. Science **281:**1197–1200.
55. **Scolnik, P. A., M. A. Walker, and B. L. Marrs.** 1980. Biosynthesis of carotenoids derived from neurosporene in *Rhodopseudomonas capsulata*. J. Biol. Chem. **255:**2427–2432.
56. **Setterdahl, A. T., B. S. Goldman, M. Hirasawa, P. Jacquot, A. J. Smith, R. G. Kranz, and D. B. Knaff.** 2000. Oxidation-reduction properties of disulfide-containing proteins of the *Rhodobacter capsulatus* cytochrome *c* biogenesis system. Biochemistry **39:**10172–10176.
57. **Sistrom, W. R.** 1960. A requirement for sodium in the growth of *Rhodopseudomonas sphaeroides*. J. Gen. Microbiol. **22:**778–785.
58. **Thomas, P. E., D. Ryan, and W. Levin.** 1976. An improved staining procedure for the detection of the peroxidase activity of cytochrome P-450 on sodium dodecyl sulfate polyacrylamide gels. Anal. Biochem. **75:**168–176.
59. **Thony-Meyer, L.** 1997. Biogenesis of respiratory cytochromes in bacteria. Microbiol. Mol. Biol. Rev. **61:**337–376.
60. **Thony-Meyer, L.** 2002. Cytochrome *c* maturation: a complex pathway for a simple task? Biochem. Soc. Trans. **30:**633–638.
61. **Thony-Meyer, L.** 2000. Haem-polypeptide interactions during cytochrome *c* maturation. Biochim. Biophys. Acta **1459:**316–324.
62. **Yano, T., C. Sanders, J. Catalano, and F. Daldal.** 2005. 5-FOA/*pyrE* based bi-directional auxotrophic selection system of *Rhodobacter capsulatus*: Construction of an unmarked mutant in the *helC* gene. Appl. Environ. Microbiol. **71:**3014–3024.
63. **Yen, H. C., N. T. Hu, and B. L. Marrs.** 1979. Characterization of the gene transfer agent made by an overproducer mutant of *Rhodopseudomonas capsulata*. J. Mol. Biol. **131:**157–168.
64. **Yen, H. C., and B. L. Marrs.** 1976. Map of genes for the carotenoid and bacteriochlorophyll biosynthesis in *Rhodopseudomonas capsulata*. J. Bacteriol. **126:**619–629.
65. **Yeoman, K. H., M. J. Delgado, M. Wexler, J. A. Downie, and A. W. Johnston.** 1997. High affinity iron acquisition in *Rhizobium leguminosarum* requires the *cycHJKL* operon and the *feuPQ* gene products, which belong to the family of two-component transcriptional regulators. Microbiology **143:**127–134.
66. **Zannoni, D., and F. Daldal.** 1993. The role of *c*-type cytochromes in catalyzing oxidative and photosynthetic electron transport in the dual functional plasma membrane of facultative phototrophs. Arch. Microbiol. **160:**413–423.